Propagation and Localization of Collective Excitations on a 24-Qubit Superconducting Processor

Yangsen Ye,[1,2,*] Zi-Yong Ge,[3,4,*] Yulin Wu,[1,2,*] Shiyu Wang,[1,2] Ming Gong,[1,2] Yu-Ran Zhang,[5,6] Qingling Zhu,[1,2] Rui Yang,[1,2] Shaowei Li,[1,2] Futian Liang,[1,2] Jin Lin,[1,2] Yu Xu,[1,2] Cheng Guo,[1,2] Lihua Sun,[1,2] Chen Cheng,[7,5] Nvsen Ma,[3] Zi Yang Meng,[3,4,8,9] Hui Deng,[1,2] Hao Rong,[1,2] Chao-Yang Lu,[1,2] Cheng-Zhi Peng,[1,2] Heng Fan,[3,4,8,9,†] Xiaobo Zhu,[1,2,‡] and Jian-Wei Pan[1,2]

[1]*Hefei National Laboratory for Physical Sciences at Microscale and Department of Modern Physics, University of Science and Technology of China, Hefei, Anhui 230026, China*

[2]*Shanghai Branch, CAS Center for Excellence and Synergetic Innovation Center in Quantum Information and Quantum Physics, University of Science and Technology of China, Shanghai 201315, China*

[3]*Beijing National laboratory for Condensed Matter Physics, Institute of Physics, Chinese Academy of Sciences, Beijing 100190, China*

[4]*School of Physical Sciences, University of Chinese Academy of Sciences, Beijing 100190, China*

[5]*Beijing Computational Science Research Center, Beijing 100193, China*

[6]*Theoretical Quantum Physics Laboratory, RIKEN Cluster for Pioneering Research, Wako-shi, Saitama 351-0198, Japan*

[7]*Center of Interdisciplinary Studies, Lanzhou University, Lanzhou 730000, China*

[8]*CAS Center for Excellence in Topological Quantum Computation, UCAS, Beijing 100190, China*

[9]*Songshan Lake Materials Laboratory, Dongguan 523808, China*

(Received 7 May 2019; published 30 July 2019)

Superconducting circuits have emerged as a powerful platform of quantum simulation, especially for emulating the dynamics of quantum many-body systems, because of their tunable interaction, long coherence time, and high-precision control. Here in experiments, we construct a Bose-Hubbard ladder with a ladder array of 20 qubits on a 24-qubit superconducting processor. We investigate theoretically and demonstrate experimentally the dynamics of single- and double-excitation states with distinct behaviors, indicating the uniqueness of the Bose-Hubbard ladder. We observe the linear propagation of photons in the single-excitation case, satisfying the Lieb-Robinson bounds. The double-excitation state, initially placed at the edge, localizes; while placed in the bulk, it splits into two single-excitation modes spreading linearly toward two boundaries, respectively. Remarkably, these phenomena, studied both theoretically and numerically as unique properties of the Bose-Hubbard ladder, are represented coherently by pairs of controllable qubits in experiments. Our results show that collective excitations, as a single mode, are not free. This work paves the way to simulation of exotic logic particles by subtly encoding physical qubits and exploration of rich physics by superconducting circuits.

DOI: 10.1103/PhysRevLett.123.050502

The dynamics of quantum many-body systems have attracted a lot of interest in recent years [1]. In addition to the conventional equilibrium physics, nonequilibrium systems have abundant unique phenomena, which require new theoretical and experimental research tools. For a clean system with a local Hamiltonian, the propagation of information shows light-cone-like spreading limited by Lieb-Robinson bounds [2]. Nevertheless, when sufficiently strong disorder is applied to the systems, the quasiparticles may be localized. Examples include the Anderson localization [3] in noninteracting systems, and many-body localization in interacting systems [4]. In the topological systems, the localization can also emerge at the edges without impurities [5–8]. To explore the dynamics of quantum many-body systems, i.e., quantum simulation [9,10], synthetic quantum systems provide a well-controlled platform, owing to the ability of precise control of tunable interactions and intrinsic dynamical process. Moreover, superconducting circuits [11,12], as a scalable system for quantum computation, have been applied to many quantum-simulation experiments, e.g., digital dynamical simulations [13,14], many-body localization [15,16], quantum chemistry [17,18], topological phases [19–21], and demonstrations of various quantum algorithms [22–27].

The Bose-Hubbard model [28,29], one of the most prominent models in condensed matter physics, embraces rich underlying physics of strong correlated systems, and has been investigated experimentally in optical lattices [30] and circuit quantum electrodynamics [12,31]. Many novel dynamical phenomena of the Bose-Hubbard model have been observed in 1D and 2D systems, such as the dynamical behaviors of quantum phase transitions between the superfluid and Mott insulators [32,33], the localization with disordered local potentials [16], the stabilization of

Mott insulators [34], and quantum walks [35–37]. Different from the 1D case, the Bose-Hubbard ladder can show unique emergent effects, especially, topological effects, which have been studied both theoretically and experimentally [38–40]. However, the dynamics of the Bose-Hubbard ladder model are not studied extensively. Thus, we would like to ask whether there are any special dynamical properties in the ladder model, which are distinct to the 1D case.

In this Letter, we experimentally demonstrate a Bose-Hubbard ladder, using 20 qubits on two legs of a 24-qubit ladder superconducting processor, and investigate the dynamics of the single- and double-excitation modes. For the single-excitation case, we find it similar to a 1D chain, displaying the linear propagation [35–37] limited by Lieb-Robinson bounds. For the double-excitation case, we observe the localization of boundary collective excitations, which is a unique property of the Bose-Hubbard ladder. However, we find that the double-excitation mode is not stable in the bulk; instead, it splits into two single-excitation modes spreading linearly towards both sides, respectively. These phenomena show that the Bose-Hubbard ladder is not equivalent to the free-fermion system in the large-U regime, which is distinct to the 1D Bose-Hubbard chain. They will also help us further understand the mechanism and the nonequilibrium behaviors of strongly correlated many-body systems. The experimental observation of the distinctions between bulk and edge depends on that the ladder should be long enough. Our 20-qubit ladder of superconducting device satisfies this condition, and the boundary effects can be clearly identified. Furthermore, our experimental platform enables us to explore many other interesting topics in quantum computation and quantum simulations in different structures of lattices.

Our superconducting circuits, shown schematically in Fig. 1(a), can be described by the Bose-Hubbard ladder with a Hamiltonian ($\hbar = 1$)

$$H = \sum_{j\nu} J_{j\nu}(\hat{a}^{\dagger}_{j\nu}\hat{a}_{(j+1)\nu} + \text{H.c.}) + \sum_{j} J_{jR}(\hat{a}^{\dagger}_{jA}\hat{a}_{jB} + \text{H.c.}) + \frac{U}{2}\sum_{j\nu}\hat{n}_{j\nu}(\hat{n}_{j\nu} - 1) + \sum_{j\nu} h_{j\nu}\hat{n}_{j\nu}, \quad (1)$$

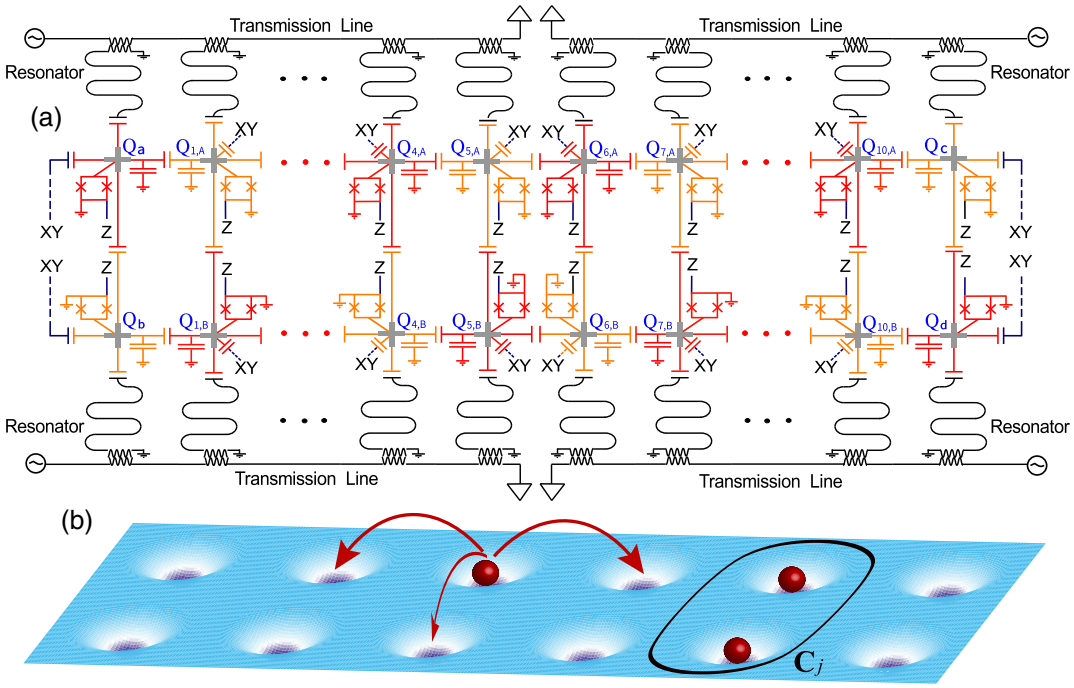

FIG. 1. Experimental setup. (a) Circuit diagram of the device. There are 24 superconducting transmon qubits (Q_{1A}-Q_{10A}, Q_{1B}-Q_{10B} and Q_a-Q_d) constituting a ladder [41–45]. The nearest-neighbor hopping is realized by the capacitive coupling between qubits, and the negative anharmonicity U of each qubit gives the on-site attractive interaction. The frequency of each qubit is tunable by individual microwave driving through the flux-bias line. Readout resonators are separated into four groups, and the resonators in each group share a microwave transmission line for multiplexed readout. More experimental details of our system are presented in the Supplemental Material [46]. In our experiments, the middle 20 qubits (Q_{1A}-Q_{10A}, Q_{1B}-Q_{10B}) are biased to the working frequency 4.8 GHz. The other four qubits (Q_a-Q_d) are always idled with frequencies 3.5, < 3.5, 5.4, and < 3 GHz, respectively. Thus, Q_a-Q_d are far away from the working frequency, and thus, a 20-qubit ladder is employed. (b) The image of the corresponding Bose-Hubbard ladder with 6 rungs. The red ball represents the photon (the excitation of the qubit), which can tunnel to the nearest-neighbor sites (red arrows). We label two qubits, which share the same rung (black box), as a unit cell C_j.

where j denotes the number of rung, $\nu = A/B$ denotes the leg A/B, $\hat{a}^{\dagger}_{j\nu}$ ($\hat{a}_{j\nu}$) is the bosonic creation (annihilation) operator, $\hat{n}_{j\nu} \equiv \hat{a}^{\dagger}_{j\nu}\hat{a}_{j\nu}$ is the number operator, $h_{j\nu}$ is the tunable local field strength, set to be the same during the quench dynamics, U is the on-site interaction, $J_{j\nu}$ is the nearest-neighbor coupling strength of the leg ν, and J_{jR} is the coupling strength of two qubits at the rung j. The excitation in the superconducting qubit can be regarded as a photon in the microwave regime [16,35]. For convenience, we regard two sites, which share the same rung, i.e., Q_{jA} and Q_{jB}, as a unit cell labeled as C_j, with $j = 1, \ldots, 10$. Then, this system can also be taken as a quasi-1D model, see Fig. 1(b).

In our superconducting circuits, the nearest-neighbor hopping strength $J_{j\nu}/2\pi \simeq J_{jR}/2\pi \simeq 12$ MHz, and the anharmonicity $U/2\pi \simeq -230$ MHz. Because $|U|/J_{j\nu} \simeq 19 \gg 1$, two photons can hardly bunch at the same site, indicating that the photons in this system behave as hard-core bosons. Therefore, the state of C_j can be approximatively expanded by four basis $|00\rangle_j$, $|01\rangle_j \equiv \hat{a}^{\dagger}_{jB}|00\rangle_j$, $|10\rangle_j \equiv \hat{a}^{\dagger}_{jA}|00\rangle_j$, and $|11\rangle_j \equiv \hat{a}^{\dagger}_{jA}\hat{a}^{\dagger}_{jB}|00\rangle_j$, where $|00\rangle_j$ is the vacuum state, representing that there is no photon at C_j. Here, we regard $|01\rangle_j$ and $|10\rangle_j$ as single-excitation states, and $|11\rangle_j$ as the double-excitation state. In this case, the nonlinear term of H in Eq. (1) vanishes, and the system reduces to a single-particle problem. Thus, with $J_{jA} \simeq J_{jB}$ assumed, we can write an effective Hamiltonian of H as [46]

$$H_{\mathrm{eff}} = \sum_{j=1}^{10} \tilde{J}_j(\hat{d}^{\dagger}_j\hat{d}_{j+1} + \hat{f}^{\dagger}_j\hat{f}_{j+1} + \mathrm{H.c.}) + \sum_{j=1}^{10} \mu_j(\hat{d}^{\dagger}_j\hat{d}_j - \hat{f}^{\dagger}_j\hat{f}_j), \tag{2}$$

where $\hat{d}_j \equiv (\hat{a}_{jA} + \hat{a}_{jB})/\sqrt{2}$, $\hat{f}_j \equiv (\hat{a}_{jA} - \hat{a}_{jB})/\sqrt{2}$, $\tilde{J}_j \equiv (J_{jA} + J_{jB})/2$, and $\mu_j \equiv J_{jR}$. Then, we can find that there are two decoupled free modes in the system. Moreover, note that with the qubit representation, $\hat{d}^{\dagger}_j|00\rangle_j = (|10\rangle_j + |01\rangle_j)/\sqrt{2}$ and $\hat{f}^{\dagger}_j|00\rangle_j = (|10\rangle_j - |01\rangle_j)/\sqrt{2}$ are triplet state and singlet state, respectively.

First, we investigate the quench dynamics of the system with single-excitation initial states. During the time evolution, we measure the probability distribution of the single-excitation state, $P^{\mathrm{se}}_j \equiv P^{01}_j + P^{10}_j$, by simultaneous single-shot readouts of two qubits at C_j, where P^{01}_j and P^{10}_j are the probabilities of single-excitation states $|01\rangle_j$ and $|10\rangle_j$ of C_j, respectively. In Figs. 2(a) and 2(b), we prepare a single-excitation state $|10\rangle_1$ localized at the left edge (C_1) and $|10\rangle_6$ at the central of the bulk (C_6), by exciting the corresponding qubits after the system's initialization. In Fig. 2(c), we prepare a state $|10\rangle_1 \otimes |01\rangle_{10}$ with two single excitations localized at both edges (C_1 and C_{10}). For these three cases, we observe the linear propagation of single excitations. In Figs. 2(d)–2(f), we compare the corresponding ideally theoretical predictions with experimental data in Figs. 2(a)–2(c). The experimental results agree well with the theoretical predictions.

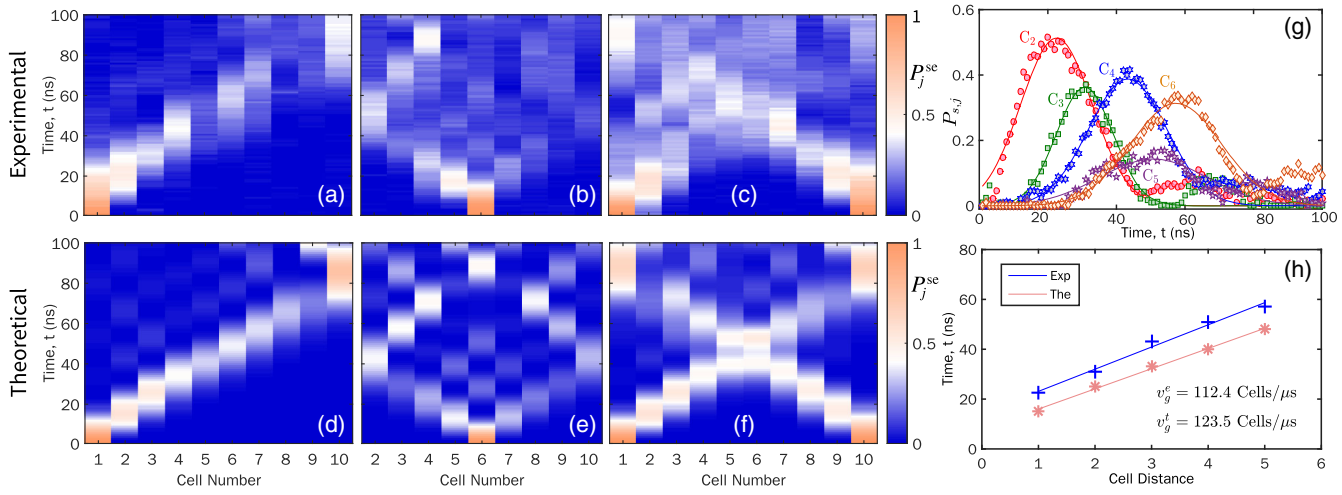

FIG. 2. Time evolutions of single-excitation states up to 100 ns. Time evolutions of the probability distributions of single excitations P^{se}_j starting with one initial single-excitation state $|10\rangle_1$ and $|10\rangle_6$ at (a) the leftmost cell C_1 and (b) the central cell C_6, and the states $|10\rangle_1 \otimes |01\rangle_{10}$ of two initial single excitations at (c) C_1 and C_{10}, respectively, are shown. For (b), C_1 is at the idle frequency to be turned off to make C_6 central. (d)–(f) are for the corresponding numerical results for comparisons with (a)–(c). In the numerical simulation, decoherence is not considered, and the experimental parameters are used. (g) Time evolutions of the probability distributions of (a) for C_2–C_6. The scattering points are experimental data, while the solid curves are for the corresponding Gaussian fitting analysis. (h) The linear fitting analysis of (g) between the time of the first peak of the probability distribution and the cell distance. The experimental data (blue cross) are obtained from the Gaussian fitting curves, while the theoretical ones (orange stars) are obtained from the numerical results. We calculate the experimental group velocity as $v^{\mathrm{Ex}}_g = 112.4$ cells/μs, and theoretic one as $v^{\mathrm{Th}}_g = 123.5$ cells/μs.

In the single-particle representation, the effective Hamiltonian in Eq. (2) describes two decoupled 1D free hardcore-boson systems. These two free modes are both linear combinations of two single-excitation states, corresponding to the Bell states of two qubits. Hence, the propagation of a single excitation is linear and limited by the Lieb-Robinson bounds [2] with the maximal group speed $v_g^{\max} = 145.9$ cells/μs [46,47], see Fig. 2(g). To extract the group propagation velocity v_g of the single excitation, we use the linear fitting between the time of the first probability peak and the cell distance, as shown in Fig. 2(h). The experimental group velocity is $v_g^{\mathrm{Ex}} = 112.4$ cells/μs, and the theoretical one is $v_g^{\mathrm{Th}} = 123.5$ cells/μs by using device parameters, between which the difference may result from unbalanced qubits' frequencies during the experiments.

Then, we study the dynamics of double excitations, starting with only one double-excitation initial state $|11\rangle_j$ at C_j after system initialization. In Figs. 3(a) and 3(b), theoretical and experimental evolutions of the probability distributions of double-excitation states P_j^{11} for qubit-qubit unit cells are shown, where the initial double-excitation state is localized at the leftmost cell (C_1). By analyzing the distributions P_j^{11}, we can find that the evolution of the double-excitation state displays boundary localization, which is quite distinct from the case of the single-excitation states. When the initial double-excitation state is in the bulk, e.g., at the central cell (C_6) as shown in Figs. 3(c) and 3(d), we can observe no localization. Instead, this double-excitation state splits into two independent single-excitation modes, spreading linearly toward two edges, respectively, see Figs. 3(e) and 3(f), which shows photons' antibunching.

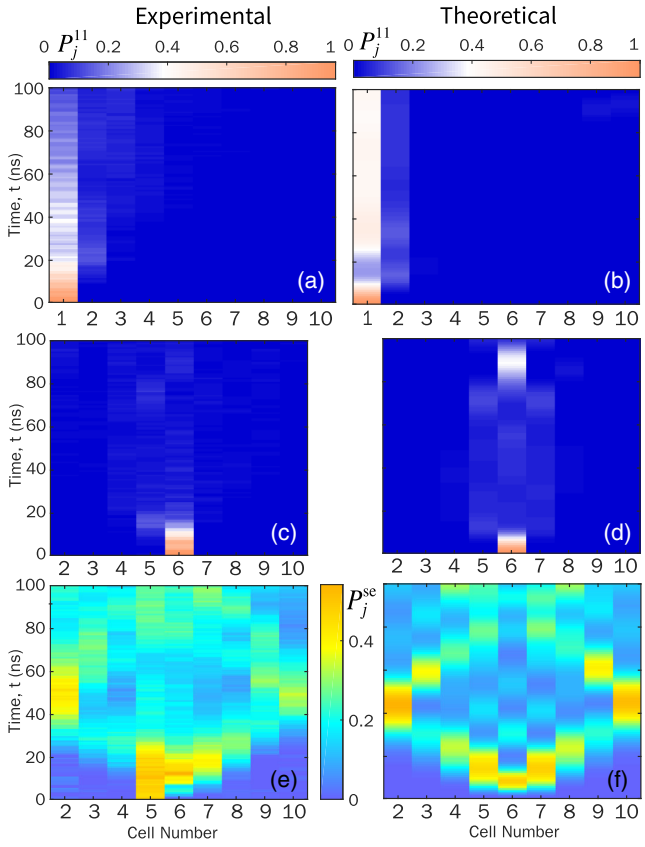

FIG. 3. Time evolutions of double-excitation states up to 100 ns. Time evolutions of the probability distributions of double excitations P_j^{11} with initial double-excitation states $|11\rangle_1$ and $|11\rangle_6$ at: (a),(b) C_1 and (c),(d) C_6, respectively, are plotted. In (a) and (c), experimental results are shown; in (b) and (d), corresponding numerical results are shown. Similarly, C_1 is at the idle frequency to be turned off for the central localized initial state in (c),(d). The (e) experimental and (f) theoretical evolutions of the probability distributions of single excitations P_j^{se} for the central localized initial state in (c),(d) are shown, respectively.

In our system, since the large-U condition is satisfied, the photons can exhibit fermionization and behave like free fermions, implying negligible double occupancy at a single qubit. However, the edge localization of the double-excitation state cannot be described by free fermions [46]. In contrast to the single-excitation case, the dynamics of the double-excitation states cannot be described by the single-particle representation, and the correlation of two modes neglected in Eq. (2) should be considered. In fact, in the large-U limit, the Bose-Hubbard model more likely conforms to the XX spin systems. In the Supplemental Material [46], we present a phenomenological interpretation of the double-excitation dynamics in the perspective of the XX spin ladder.

Then, to see how the on-site interaction strength U affects the edge state localization, we present in Fig. 4 the numerical results of the dynamics of the ideal

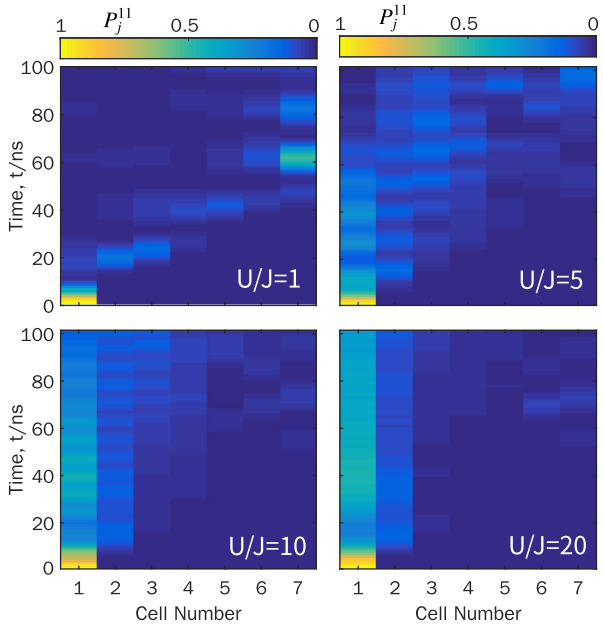

FIG. 4. Numerical results of time evolutions up to 100 ns of the double-excitation states of 7 cells for different regimes of interaction strength with initial double-excitation states at C_1. Here, we choose $J/2\pi = 12$ MHz, and $U/J = 1, 5, 10, 20$, respectively.

Bose-Hubbard ladder ($J_{jA} = J_{jB} = J_{jR} = J$) for different regimes of interaction strength. We find that the edge localization of double-excitation states can only exist in the large-U regime. The edge localization disappears in the small-U regime, because of large probabilities of bosons' bunching at the same sites [46], which can further show that the edge localization results from the interactions.

In addition, we study the correlation functions of the ground states of the XX spin ladder by the density matrix renormalization group (DMRG) methods [46]. The simulation results clearly reveal that for the double excitations, their edge correlations decay much faster than that of the bulk, and this different scaling behavior shows that the ground state also has the similar boundary effects. This is a phenomenon, absent from free-fermion systems but rooted in the interaction effect, and our 20-qubit experimental system can really capture it.

In conclusion, we have theoretically and experimentally studied the quench dynamics of the Bose-Hubbard ladder on the superconducting circuits. Benefiting from the precise control and readout of a 24-qubit superconducting quantum processor, we directly observe (i) the linear propagation of single excitations, (ii) the localization of the edge double excitations, and (iii) the instability of bulk double excitations with a 20-qubit ladder. Our experiments show that collective excitations are not free on the Bose-Hubbard ladder, which cannot be described in the single-particle picture. Our results may be useful for further studies on the statistical properties of particles in strongly correlated systems. Moreover, in addition to recent work on the Bose-Hubbard chains [35], our platform provides the possibilities for further explorations of the distinctions between chain and ladder models, e.g., magnon scattering, the scaling of correlation functions, and entanglement entropies [48–50].

This work was partially carried out at the USTC Center for Micro and Nanoscale Research and Fabrication. This research was supported by the National Basic Research Program (973) of China (Grant No. 2017YFA0304300), the Chinese Academy of Sciences, Anhui Initiative in Quantum Information Technologies, Technology Committee of Shanghai Municipality, NSFC (Grants No. 11574380, No. 11774406, No. U1530401). National Key Research and Development Program of China (Grant No. 2016YFA0302104, No. 2016YFA0300600), Strategic Priority Research Program of Chinese Academy of Sciences (Grant No. XDB28000000), China Postdoctoral Science Foundation (Grant No. 2018M640055), and Beijing Science Foundation (Grant No. Y18G07). The authors also thank QuantumCTek Co., Ltd. for supporting the fabrication and the maintenance of room temperature electronics.

*These authors contributed equally to this work.
†hfan@iphy.ac.cn
‡xbzhu16@ustc.edu.cn

[1] J. Eisert, M. Friesdorf, and C. Gogolin, Quantum many-body systems out of equilibrium, Nat. Phys. **11**, 124 (2015).
[2] E. H. Lieb and D. W. Robinson, The finite group velocity of quantum spin systems, Commun. Math. Phys. **28**, 251 (1972).
[3] P. W. Anderson, Absence of diffusion in certain random lattices, Phys. Rev. **109**, 1492 (1958).
[4] D. M. Basko, I. L. Aleiner, and B. L. Altshuler, Metal-insulator transition in a weakly interacting many-electron system with localized single-particle states, Ann. Phys. (Amsterdam) **321**, 1126 (2006).
[5] M. Z. Hasan and C. L. Kane, Colloquium: Topological insulators, Rev. Mod. Phys. **82**, 3045 (2010).
[6] X. L. Qi and S. C. Zhang, Topological insulators and superconductors, Rev. Mod. Phys. **83**, 1057 (2011).
[7] A. Bansil, H. Lin, and T. Das, Colloquium: Topological band theory, Rev. Mod. Phys. **88**, 021004 (2016).
[8] C. K. Chiu, J. C. Y. Teo, A. P. Schnyder, and S. Ryu, Classification of topological quantum matter with symmetries, Rev. Mod. Phys. **88**, 035005 (2016).
[9] I. Buluta and F. Nori, Quantum simulators, Science **326**, 108 (2009).
[10] I. M. Georgescu, S. Ashhab, and F. Nori, Quantum simulation, Rev. Mod. Phys. **86**, 153 (2014).
[11] Y. Makhlin, G. Schön, and A. Shnirman, Quantum-state engineering with Josephson-junction devices, Rev. Mod. Phys. **73**, 357 (2001).
[12] X. Gu, A. F. Kockum, A. Miranowicz, Y. Liu, and F. Nori, Microwave photonics with superconducting quantum circuits, Phys. Rep. **718**, 1 (2017).
[13] Y. Salathé, M. Mondal, M. Oppliger, J. Heinsoo, P. Kurpiers, A. Potočnik, A. Mezzacapo, U. Las Heras, L. Lamata, E. Solano, S. Filipp, and A. Wallraff, Digital Quantum Simulation of Spin Models with Circuit Quantum Electrodynamics, Phys. Rev. X **5**, 021027 (2015).
[14] R. Barends *et al.*, Digital quantum simulation of fermionic models with a superconducting circuit, Nat. Commun. **6**, 7654 (2015).
[15] K. Xu, J. J. Chen, Y. Zeng, Y. R. Zhang, C. Song, W. X. Liu, Q. J. Guo, P. F. Zhang, D. Xu, H. Deng, K. Q. Huang, H. Wang, X. B. Zhu, D. N. Zheng, and H. Fan, Emulating Many-Body Localization with a Superconducting Quantum Processor, Phys. Rev. Lett. **120**, 050507 (2018).
[16] P. Roushan *et al.*, Spectroscopic signatures of localization with interacting photons in superconducting qubits, Science **358**, 1175 (2017).
[17] P. J. J. O'Malley *et al.*, Scalable Quantum Simulation of Molecular Energies, Phys. Rev. X **6**, 031007 (2016).
[18] A. Kandala, A. Mezzacapo, K. Temme, M. Takita, M. Brink, J. M. Chow, and J. M. Gambetta, Hardware-efficient variational quantum eigensolver for small molecules and quantum magnets, Nature (London) **549**, 242 (2017).
[19] Y. P. Zhong, D. Xu, P. Wang, C. Song, Q. J. Guo, W. X. Liu, K. Xu, B. X. Xia, C.-Y. Lu, S. Han, J.-W. Pan, and H. Wang, Emulating Anyonic Fractional Statistical Behavior in a Superconducting Quantum Circuit, Phys. Rev. Lett. **117**, 110501 (2016).
[20] C. Song, D. Xu, P. Zhang, J. Wang, Q. Guo, W. Liu, K. Xu, H. Deng, K. Huang, D. Zheng, S.-B. Zheng, H. Wang, X. Zhu, C.-Y. Lu, and J.-W. Pan, Demonstration of Topological

Robustness of Anyonic Braiding Statistics with a Superconducting Quantum Circuit, Phys. Rev. Lett. **121**, 030502 (2018).

[21] E. Flurin, V. V. Ramasesh, S. Hacohen-Gourgy, L. S. Martin, N. Y. Yao, and I. Siddiqi, Observing Topological Invariants using Quantum Walks in Superconducting Circuits, Phys. Rev. X **7**, 031023 (2017).

[22] E. Lucero, R. Barends, Y. Chen, J. Kelly, M. Mariantoni, A. Megrant, P. OMalley, D. Sank, A. Vainsencher, J. Wenner, T. White, Y. Yin, A. N. Cleland, and J. M. Martinis, Computing prime factors with a Josephson phase qubit quantum processor, Nat. Phys. **8**, 719 (2012).

[23] M. Gong *et al.*, Genuine 12-Qubit Entanglement on a Superconducting Quantum Processor, Phys. Rev. Lett. **122**, 110501 (2019).

[24] R. Barends *et al.*, Digitized adiabatic quantum computing with a superconducting circuit, Nature (London) **534**, 222 (2016).

[25] Y. Zheng, C. Song, M. C. Chen, B. Xia, W. Liu, Q. Guo, L. Zhang, D. Xu, H. Deng, K. Huang, Y. Wu, Z. Yan, D. Zheng, L. Lu, J. W. Pan, H. Wang, C. Y. Lu, and X. Zhu, Solving Systems of Linear Equations with a Superconducting Quantum Processor, Phys. Rev. Lett. **118**, 210504 (2017).

[26] C. Song, K. Xu, W. X. Liu, C. P. Yang, S. B. Zheng, H. Deng, Q. W. Xie, K. Q. Huang, Q. J. Guo, L. B. Zhang, P. F. Zhang, D. Xu, D. N. Zheng, X. B. Zhu, H. Wang, Y. A. Chen, C. Y. Lu, S. Y. Han, and J. W. Pan, 10-Qubit Entanglement and Parallel Logic Operations with a Superconducting Circuit, Phys. Rev. Lett. **119**, 180511 (2017).

[27] C. Song, K. Xu, H. Li, Y. Zhang, X. Zhang, W. Liu, Q. Guo, Z. Wang, W. Ren, J. Hao, H. Feng, H. Fan, D. Zheng, D. Wang, H. Wang, and S. Zhu, Observation of multi-component atomic Schrödinger cat states of up to 20 qubits, arXiv:1905.00320.

[28] M. P. A. Fisher, P. B. Weichman, G. Grinstein, and D. S. Fisher, Boson localization and the superfluid-insulator transition, Phys. Rev. B **40**, 546 (1989).

[29] M. A. Cazalilla, R. Citro, T. Giamarchi, E. Orignac, and M. Rigol, One dimensional bosons: From condensed matter systems to ultracold gases, Rev. Mod. Phys. **83**, 1405 (2011).

[30] D. Jaksch, C. Bruder, J. I. Cirac, C. W. Gardiner, and P. Zoller, Cold Bosonic Atoms in Optical Lattices, Phys. Rev. Lett. **81**, 3108 (1998).

[31] S. Hacohen-Gourgy, V. V. Ramasesh, C. De Grandi, I. Siddiqi, and S. M. Girvin, Cooling and Autonomous Feedback in a Bose-Hubbard Chain with Attractive Interactions, Phys. Rev. Lett. **115**, 240501 (2015).

[32] M. Greiner, O. Mandel, T. Esslinger, T. W. Hänsch, and I. Bloch, Quantum phase transition from a superfluid to a Mott insulator in a gas of ultracold atoms, Nature (London) **415**, 39 (2002).

[33] M. Greiner, O. Mandel, T. W. Hänsch, and I. Bloch, Collapse and revival of the matter wave field of a Bose-Einstein condensate, Nature (London) **419**, 51 (2002).

[34] R. Ma, B. Saxberg, C. Owens, N. Leung, Y. Lu, J. Simon, and D. I. Schuster, A dissipatively stabilized Mott insulator of photons, Nature (London) **566**, 51 (2019).

[35] Z. Yan, Y. R. Zhang, M. Gong, Y. Wu, Y. Zheng, S. Li, C. Wang, F. Liang, J. Lin, Y. Xu, C. Guo, L. Sun, C. Z. Peng, K. Xia, H. Deng, H. Rong, J. Q. You, F. Nori, H. Fan, X. Zhu, and J.-W. Pan, Strongly correlated quantum walks with a 12-qubit superconducting processor, Science **364**, 753 (2019).

[36] M. Cheneau, P. Barmettler, D. Poletti, M. Endres, P. Schau, T. Fukuhara, C. Gross, I. Bloch, C. Kollath, and S. Kuhr, Light-cone-like spreading of correlations in a quantum many-body system, Nature (London) **481**, 484 (2012).

[37] P. M. Preiss, R. Ma, M. E. Tai, A. Lukin, M. Rispoli, P. Zupancic, Y. Lahini, R. Islam, and M. Greiner, Strongly correlated quantum walks in optical lattices, Science **347**, 1229 (2015).

[38] E. Orignac and T. Giamarchi, Meissner effect in a bosonic ladder, Phys. Rev. B **64**, 144515 (2001).

[39] A. Petrescu and K. L. Hur, Bosonic Mott Insulator with Meissner Currents, Phys. Rev. Lett. **111**, 150601 (2013).

[40] M. Atala, M. Aidelsburger, M. Lohse, J. T. Barreiro, B. Paredes, and I. Bloch, Observation of chiral currents with ultracold atoms in bosonic ladders, Nat. Phys. **10**, 588 (2014).

[41] J. Q. You, X. Hu, S. Ashhab, and F. Nori, Low-decoherence flux qubit, Phys. Rev. B **75**, 140515(R) (2007).

[42] J. Koch, T. M. Yu, J. Gambetta, A. A. Houck, D. I. Schuster, J. Majer, A. Blais, M. H. Devoret, S. M. Girvin, and R. J. Schoelkopf, Charge-insensitive qubit design derived from the Cooper pair box, Phys. Rev. A **76**, 042319 (2007).

[43] R. Barends, J. Kelly, A. Megrant, A. Veitia, D. Sank, E. Jeffrey, T. C. White, J. Mutus, A. G. Fowler, B. Campbell, Y. Chen, Z. Chen, B. Chiaro, A. Dunsworth, C. Neill, P. O'Malley, P. Roushan, A. Vainsencher, J. Wenner, A. N. Korotkov, A. N. Cleland, and J. M. Martinis, Superconducting quantum circuits at the surface code threshold for fault tolerance, Nature (London) **508**, 500 (2014).

[44] J. Y. Mutus, T. C. White, R. Barends, Yu Chen, Z. Chen, B. Chiaro, A. Dunsworth, E. Jeffrey, J. Kelly, A. Megrant, C. Neill, P. J. J. O'Malley, P. Roushan, D. Sank, A. Vainsencher, J. Wenner, K. M. Sundqvist, A. N. Cleland, and John M. Martinis, Strong environmental coupling in a Josephson parametric amplifier, Appl. Phys. Lett. **104**, 263513 (2014).

[45] E. Lucero, J. Kelly, R. C. Bialczak, M. Lenander, M. Mariantoni, M. Neeley, A. D. O'Connell, D. Sank, H. Wang, M. Weides, J. Wenner, T. Yamamoto, A. N. Cleland, and J. M. Martinis, Reduced phase error through optimized control of a superconducting qubit, Phys. Rev. A **82**, 042339 (2010).

[46] See Supplemental Material at http://link.aps.org/supplemental/10.1103/PhysRevLett.123.050502 for the details of the experimental setup, approaches of qubit control, some theoretical derivation, and additional numerical simulation.

[47] P. Jurcevic, B. P. Lanyon, P. Hauke, C. Hempel, P. Zoller, R. Blatt, and C. F. Roos, Quasiparticle engineering and entanglement propagation in a quantum many-body system, Nature (London) **511**, 202 (2014).

[48] E. Dagotto and T. M. Rice, Surprises on the way from one- to two-dimensional quantum magnets: The ladder materials, Science **271**, 618 (1996).

[49] L. Amico, R. Fazio, A. Osterloh, and V. Vedral, Entanglement in many-body systems, Rev. Mod. Phys. **80**, 517 (2008).

[50] J. Eisert, M. Cramer, and M. B. Plenio, Colloquium: Area laws for the entanglement entropy, Rev. Mod. Phys. **82**, 277 (2010).